Original Article

Adipose mesenchymal stromal/stem cells expanded by a GMP compatible protocol displayed improved adhesion on cancer cells in flow conditions

Francesco Agostini[1], Carla Vicinanza[1], Federica Di Cintio[2,3], Monica Battiston[1], Elisabetta Lombardi[1], Giulia Golinelli[4], Cristina Durante[1], Giuseppe Toffoli[2], Massimo Dominici[4], Mario Mazzucato[1]

[1]Stem Cell Unit, [2]Experimental and Clinical Pharmacology Unit, Centro di Riferimento Oncologico di Aviano (CRO) IRCCS, Aviano (PN), Italy; [3]Department of Life Sciences, University of Trieste, Trieste, Italy; [4]Division of Medical Oncology, Laboratory of Cellular Therapies, Department of Medical and Surgical Sciences for Children & Adults, University Hospital of Modena and Reggio Emilia, Modena, Italy

Contributions: (I) Conception and design: F Agostini, M Mazzucato; (II) Administrative support: None; (III) Provision of study materials or patients: G Toffoli; (IV) Collection and assembly of data: F Agostini, C Vicinanza, F Di Cintio, M Battiston, E Lombardi, G Golinelli; (V) Data analysis and interpretation: F Agostini, C Vicinanza, C Durante, G Toffoli; (VI) Manuscript writing: All authors; (VII) Final approval of manuscript: All authors.

Correspondence to: Dr. Francesco Agostini. Centro di Riferimento Oncologico di Aviano (CRO) IRCCS, Via Franco Gallini, 2 - 33081 Aviano (PN), Italy. Email: fagostini@cro.it.

Background: Adipose tissue derived mesenchymal stromal/stem cells (ASC) can be expanded using supernatant rich in growth factors (SRGF) as Good Manufacturing Practice compatible additive, instead of fetal bovine serum (FBS). After transendothelial migration, ASC can migrate to cancer masses where they can release active substances. Due to their homing and secretion properties ASC can be used as targeted drug delivery vehicles. Nevertheless, the fraction of ASC actually reaching the tumor target is limited. The impact of culture conditions on ASC homing potential on cancer cells is unknown.

Methods: In dynamic *in vitro* conditions, we perfused FBS or SRGF ASC in flow chambers coated with collagen type I and fibronectin or seeded with endothelial cells or with HT1080, T98G and Huh7 cancer cells. Expression of selected adhesion molecules was evaluated by standard cytofluorimetry. Dynamic intracellular calcium concentration changes were evaluated in microfluidic and static conditions.

Results: When compared to FBS ASC, not specific adhesion of SRGF ASC on collagen type I and fibronectin was lower (–33.9%±12.2% and –45.3%±16.9%), while on-target binding on HT1080 and T98G was enhanced (+147%±8% and 120.5%±5.2%). Adhesion of both FBS and SRGF ASC on Huh7 cells was negligible. As confirmed by citofluorimetry and by function-blocking antibody, SRGF mediated decrease of CD49a expression accounted for lower SRGF-ASC avidity for matrix proteins. Upon stimulation with calcium ionophore in static conditions, mobilization of intracellular calcium in SRGF ASC was greater than in FBS ASC. In dynamic conditions, upon adhesion on matrix proteins and HT1080 cells, SRGF ASC showed marked oscillatory calcium concentration changes.

Conclusions: SRGF can enhance specific ASC binding capacity on selected cancer cells as HT1080 (fibrosarcoma) and T98G (glioblastoma) cells. Upon cell-cell adhesion, SRGF ASC activate intracellular responses potentially improving cell secretion functions. SRGF ASC could be considered as suitable drug delivery vehicle for cancer therapy.

Keywords: Adipose mesenchymal stromal/stem cells; Good Manufacturing Practice; homing on cancer cells; microfluidic conditions; supernatant rich in growth factors (SRGF)

Submitted Nov 27, 2019. Accepted for publication Feb 26, 2020.
doi: 10.21037/atm.2020.04.25
View this article at: http://dx.doi.org/10.21037/atm.2020.04.25

Introduction

Adipose tissue derived mesenchymal stromal/stem cells (ASC) (1) can be easily expanded applying standard tissue culture techniques. We previously published a method to isolate and expand ASC using the medium additive supernatant rich in growth factors (SRGF) derived from human platelets. Such comprehensive approach was shown (2) to be compatible with Good Manufacturing Practice (GMP) guidelines and SRGF was shown to induce a markedly faster cell proliferation when compared to the standard fetal bovine serum (FBS). ASC as well as mesenchymal stromal/stem cells (MSC) from other tissues are characterized by differentiation capacity and anti-inflammatory properties that can be harnessed for applications in regenerative medicine (3) and in immune system based diseases (4-6). Even after intravenous administration, these cells can reach primary and metastatic cancer masses (7). For such reason, autologous MSC can be exploited as vehicles to deliver a cytotoxic payload directly into the cancer mass (8,9), but the fraction of MSC actually homing to the tumor is limited (10). This drawback can reduce therapeutic efficacy of such approach. Molecular mechanisms, as well as the cascade of events leading to final MSC homing to cancer cells were not yet fully elucidated: these share close similarity to the leukocyte extravasation and tissue infiltration model (11). MSC were demonstrated to tether and roll on chemokine activated endothelium at low shear stress (0.1 dyn/cm^2) (12). Selectin ligands were shown to trigger MSC tethering and rolling on endothelial cells (12,13). Nevertheless, ASC do not express the pivotal ligand for P-selectin and a minor fraction of expanded cells was shown to roll on such substrate (14). Very Late Antigen-4 (VLA-4) i.e., the integrin dimer α4β1, composed by CD49d and CD29, is expressed by MSC and it was shown to interact with vascular cell adhesion molecule 1 (VCAM1) or CD106 in endothelial cells (12,13) thus leading to firm cell adhesion. Subsequent diapedesis followed by migration allows the final contact with target cancer cells (11). Stromal cell-derived factor-1 (SDF-1)/CXCR4 is one of the main axes governing stem cell migration and engraftment to the bone marrow following transplantation (15). Another study demonstrated that migration of ASC to cancer cells was mediated both *in vivo* and *in vitro* by the SDF-1/CXCR4 axis (16).

Calcium is a pivotal secondary signaling molecule regulating fundamental cellular functions in various cell types: intracellular calcium signaling is required to mediate adhesion of several cell types as e.g., fibroblasts (17) and platelets (18) or interaction between lymphocytes and cytokine-treated endothelial cells (19).

In this work we aimed to assess the impact of SRGF on ASC homing properties: thus, we evaluated *in vitro* ASC capacity to adhere in dynamic conditions on extracellular matrix proteins or on selected cancer cell lines. In addition, we evaluated in ASC changes of intracellular calcium concentrations occurring in static conditions or upon cell adhesion.

Methods

SRGF preparation

SRGF was prepared as previously published (2,20,21). Briefly, a platelet rich plasma obtained from single donor platelet apheresis product was added with $CaCl_2$ (Monico, Venice, Italy) at the final concentration of 0.04 M and it was incubated at 40 °C for approximately 60 min. Supernatant was separated from clot by centrifugation at 1,600 ×g for 15 min at room temperature. We used, through the whole study, a single batch of SRGF medium additive (named SRGF-CRO-2A). To manufacture the batch, we pooled together equal volumes of n=16 single donor derived SRGF products. We previously determined and validated (20) that such pool size can efficiently minimize variability between batches allowing consistent growth of ASC derived from different patients.

Cell culture

Stromal vascular fraction (SVF) cells were isolated from adipose tissue applying the protocol we previously published (2). Lipoaspirates were obtained from female breast cancer patients undergoing reconstructive lipofilling. SVF cells were frozen in autologous serum added with 5% dimethyl sulfoxide (2) until use. In order to obtain proliferating ASC, SVF cells derived from n=5 patients were separately plated in standard tissue culture flasks (BD Biosciences, Becton-Dickinson, San Jose, CA, USA). In this work we used two different media to grow ASC: Minimum Essential Medium Eagle - Alpha Modification (α-MEM) (Lonza; Basel, Switzerland) added with 10% vol/vol FBS (Lonza) or separately α-MEM added with 5% vol/vol SRGF. Both media contained 100 IU/mL of Penicillin and 100 g/mL of Streptomycin (both from Sigma, St. Louis, MO, USA).

Non-adherent cells were removed and fresh medium was added. Upon 80–90% confluence, adherent cells were detached by trypsin-ethylenediaminetetraacetic acid (EDTA) (TrypLe Select, Life Technologies-Thermo Fisher Scientific, Waltham, MA, USA). Resuspended cells were seeded at each passage at 1–2×10^3 cells/cm^2. Proliferating ASC obtained from each patient were separately expanded. On one side ASC were cultured in α-MEM medium added with 10% vol/vol FBS, while on the other side ASC were grown in α-MEM medium added with 5% SRGF. In this paper, ASC expanded in presence of 10% FBS were defined as "FBS ASC", while ASC expanded in presence of 5% SRGF were defined "SRGF ASC". Basal medium, plasticware and SRGF itself used to expand and manipulate ASC for the aims of this paper were compatible for GMP compliant production processes. Production protocol and quality controls were described in validated standard operating procedures (2). Nevertheless, cell expansion was not actually performed in a GMP approved facility for cell therapy: for such reason antibiotics were added to culture media. FBS ASC were used from passage P3 until P9 (mean population doublings at P9, 18.8±2.1), while SRGF ASC from P3 until P13 (mean population doublings at P13, 28.8±1.4). In these growth conditions, FBS and SRGF ASC were shown to be actively duplicating with unmodified proliferation rate, phenotype, differentiation potential and karyotype stability (2). When compared to FBS ASC, a higher range of population doublings was chosen for SRGF ASC considering their markedly higher proliferation potential (2): such choice was performed to compare SRGF ASC with FBS ASC in paired conditions. Both FBS ASC and SRGF ASC derived from the five different patients were used in experimental procedures performed in this work. All tests were performed in FBS and SRGF ASC derived from each donor. HT1080 (fibrosarcoma) were expanded in High glucose Dulbecco's Modified Eagle Medium (Euroclone; Milan, Italy) containing stabilized glutamine and added with 10% FBS (Lonza). T98G (glioblastoma) were cultured in Minimum Essential Medium Eagle with Earle's Salts (Euroclone) added with 1% glutamine and 10% heat inactivated FBS. Huh7 (hepatocarcinoma) cells were expanded in High glucose Dulbecco's Modified Eagle Medium containing stabilized glutamine, Non-essential amino acid mixture (Euroclone, Milan, Italy) and added with 10% FBS (Lonza). Commercially available (ThermoFisher scientific, Waltham, MA, USA) Human Umbilical Vein Endothelial Cells (HUVEC) were expanded in L200 medium added with Low Serum Growth Supplement (ThermoFisher scientific). Before confluence (80–90% covered area), cells used in this work were detached from plastic surface using trypsin-EDTA (TrypLe Select, Life Technologies-Thermo Fisher Scientific) at the appropriate dilution.

ASC adhesion on extracellular matrix proteins in microfluidic conditions

In this work we tested the potential of expanded ASC to adhere in microfluidic dynamic conditions. Experiments were performed taking advantage of a sterile disposable parallel flow chamber (ibiTreat - Slide I Luer, Ibidi GmbH, Gräfelfing, Germany). Thickness of flow chamber was 0.4 mm. Following manufacturer's instruction, the inner plastic surface was coated by the extracellular matrix proteins fibronectin (75 µg/mL) (Sigma) or collagen type I (250 µg/mL) or by the combination of both. Collagen type I was purified from commercially available bovine Achilles tendon (Sigma), following a previously published method (22). Surfaces were coated by incubation at room temperature for at least 1 hour or at +4 ℃ for 12 h. Before perfusion, flow chamber slides were connected to a syringe (BD Biosciences, Becton-Dickinson, San Jose, CA, USA) installed on a pump (Harvard Apparatus, Holliston, MA, USA) to achieve a constant flow ASC perfusion (*Figure S1*). The chamber slide was placed on an inverted epifluorescence microscope (Diaphot-TMD; Nikon, Minato, Tokyo, Japan) equipped with a bandpass filter 480/520 nm and with a digital camera (Motic 5.0, Motic, Kowloon Bay; Kowloon) controlled by Motic Images Plus 2.0 software® (*Figure S1*). ASC expanded in static conditions were detached and an appropriate amount of cells was labeled incubating the sample at 37 ℃ for 15 minutes with 10 µM carboxyfluorescein diacetate succinimidyl ester (CFDA-SE) (Vybrant® CFDA SE Cell Tracer Kit, Thermo Fisher Scientific, Waltham, MA, USA). Cells were then washed and resuspended in an appropriate volume, depending on perfusion flow rate, of α-MEM medium added with 10% vol/vol FBS and with 2% bovine serum albumin (Sigma, St. Louis, MO, USA). This was defined as "standard medium" for perfusions. Composition of the standard perfusion medium was the same when analyzing both FBS and SRGF ASC: in this way, the comparison of FBS and SRGF ASC adhesion potential was not affected by perfusion medium composition. Moreover, with this approach, we could evaluate the net impact on ASC adhesion potential in flowing conditions mediated by SRGF

addition to the cell culture medium during the expansion process. Immediately before each experimental procedure, an additional assessment of labeled cell concentration was performed. Perfusion procedures were performed at 37 ℃ in standard pCO_2 and humidity conditions. A representation of experimental procedures characterizing the ASC adhesion assay in microfluidic conditions was reported in *Figure 1A*. Labeled cells were rapidly allowed to enter and flood the chamber (bolus). Immediately after, the actual perfusion protocol was started by rapid adjustment of the flow rate selected to achieve the desired shear stress (according to manufacturer's instructions). During perfusion (15 minutes) the selected flow rate was kept constant. In order to assess cell binding kinetics, during perfusion 16 sequential images (1 picture/min) of fluorescently labeled green ASC were taken exactly on the same field. At the end of perfusion, PBS was flushed for 1 minute to remove nonspecifically bound cells. Immediately after, 13 sequential cell images of non-overlapping fields covering the entire flow chamber (from inlet to outlet) in its middle line, were taken. Then, ASC binding avidity after short-term adhesion was assessed ("adhesion strength test"): PBS was flushed at incremental steps (30 seconds each) of 0.95, 4.74, 9.48, 14.21, 17.06 dyn/cm^2. A picture of fluorescently labeled cells was taken at the end of each flow step. The number of adherent cells in each captured image was evaluated by an image processing software (Fiji Is Just ImageJ, NIH, MA, USA) (23). Modal background values were subtracted in each image using the "Math, Subtract" function. Image threshold was adjusted by default automated parameters. Thresholded images were then analyzed by the "Analyze particles" function applying pixel size range: 50-infinity pixel^2 and circularity range: 0.3–1.

In order to set up proper experimental flow conditions, we built a reference curve correlating the density of post-perfusion adherent SRGF ASC and the concentration of flowing cells at 0.25 dyn/cm^2. Experiments were performed in collagen type I coated slides. The curve and regression line analysis is shown in *Figure 1B*. In *Figure 1C*, an additional reference curve is shown correlating density of post-perfusion adherent cells and shear stress at a fixed concentration (100 cells/μL) of flowing SRGF ASC. As negative control, SRGF ASC (100 cells/μL) were perfused on uncoated chamber slides at 0.25 dyn/cm^2: the number of adherent ASC was shown to be dramatically lower (negligible) when compared to collagen type I coated slides. We selected SRGF ASC to set up experimental conditions as this kind of cells can be easily obtained in culture. We can a posteriori hypothesize that adoption of FBS ASC to generate the calibration curve could have proportionally increased the number of adherent cells on collagen type I, but minimally affecting shape or slope of the binding curve. We are confident FBS ASC were assayed in conditions comprised within reliability interval of the adopted experimental system. Similarly, we chose collagen type I to treat flow chambers for calibration tests as we could easily and abundantly purify this protein that is known to be a strong interaction substrate in dynamic conditions (24). At reduced shear stress, we hypothesized fibronectin not to significantly affect ASC binding kinetics when compared to collagen type I. Perfusions on collagen type I and fibronectin coated slides were performed at 0.1 and 0.25 dyn/cm^2 as at such shear stress levels the greatest change in adherent SRGF ASC number was shown, when compared to 0.5 dyn/cm^2. To investigate the role of CD49a in FBS and SRGF ASC adhesion to extracellular matrix proteins, a function blocking antibody specifically targeting CD49a (clone 5E8D9, Novus Biologicals, CO, USA) was used. After resuspension in the perfusion medium, labeled ASC were added with 10 μg/mL antibody and the sample was incubated for 1 hour at 37 ℃. Cell wash was not performed and ASC were perfused in parallel flow chambers that were previously coated with a mixture of collagen type I and of fibronectin. Perfusions were performed at 0.25 dyn/cm^2 shear stress. Control tests in microfluidic conditions were carried out perfusing at the same flow rate ASC that were not treated by the anti CD49a blocking antibody.

ASC adhesion on expanded cells in microfluidic conditions

Assessment of SRGF and FBS ASC adhesion potential on living expanded cells, primary HUVEC or HT1080 or Huh7 cancer cells (200–250×10^3) were seeded in the flow camera and were incubated in static conditions for at least 12 h. When appropriate, tumor necrosis factor alpha (TNF-α) at the final concentration of 50 ng/mL was added to HUVEC cells in the parallel flow chamber for 4–6 hours before perfusion. Density of adherent cells before ASC perfusion was evaluated under inverted phase contrast microscope (Olympus CKX41, Olympus Italia Srl, Milano, Italy): only parallel flow chambers containing a subconfluent cell monolayer were used for experimental procedures. ASC perfusions as well as image collection and analysis were performed following the same experimental frame described above for microfluidic tests performed on extracellular matrix proteins. As displayed

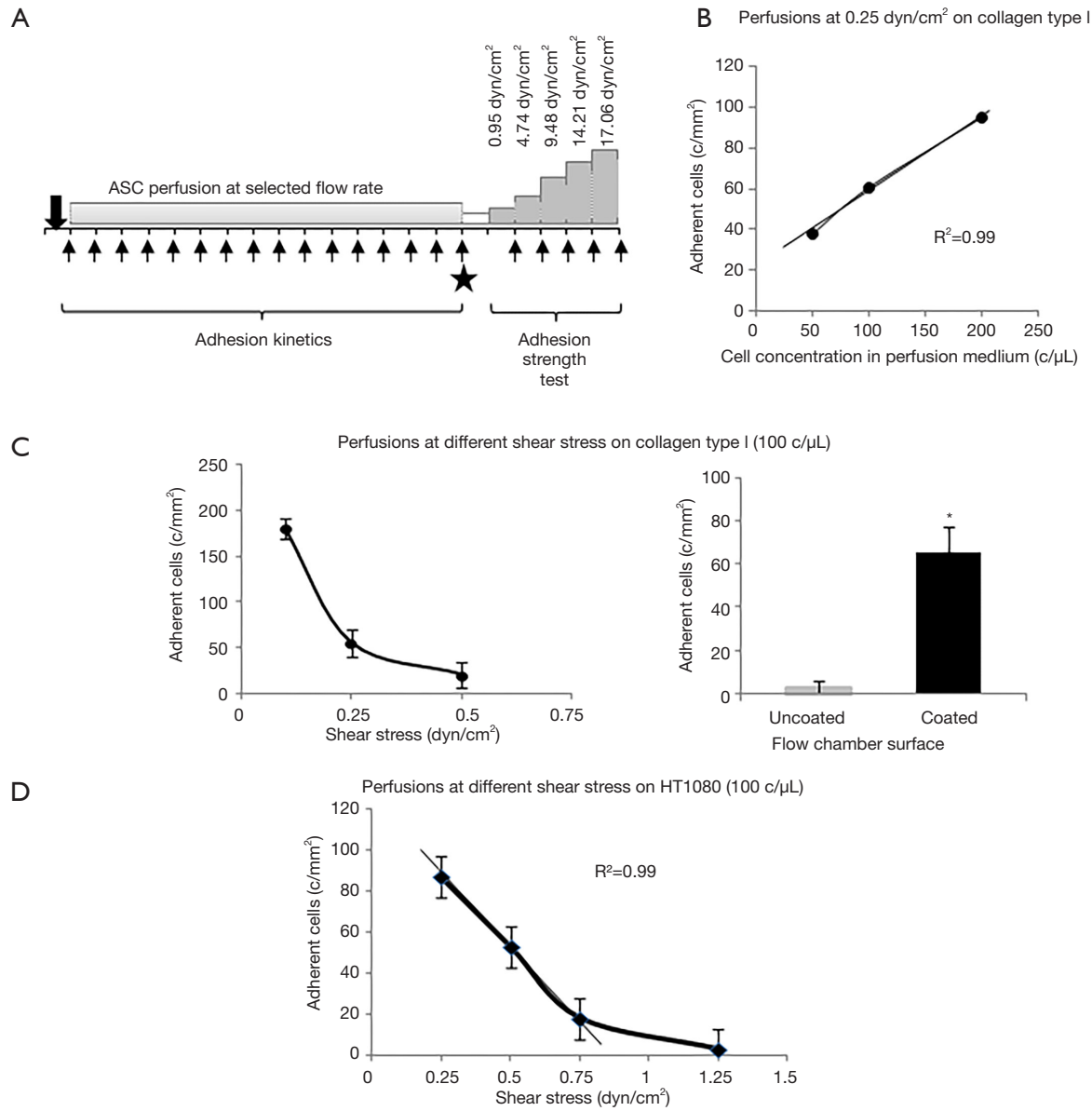

Figure 1 Schematic representation of adhesion test in dynamic conditions and preliminary assessment of experimental setup. (A) Schematic representation of ASC adhesion capacity test in flow dynamic conditions. The same test frame was applied both on matrix proteins and on primary and cancer cells. Arrows represent image acquisitions and solid star indicates post perfusion collection of pictures of adhering cells in the flow chamber; (B) reference curve describing relationships between concentration of flowing ASC at 0.25 dyn/cm^2 and adherent SRGF ASC number; (C) on the left: reference curve describing relationships between flowing ASC shear stress (at the concentration of 100 cells/µL) and the number of adhering SRGF ASC on collagen type I. SRGF ASC perfusions included in (B) and (C) were performed in standard flow medium, i.e., 10% FBS α-MEM medium added with 2% bovine serum albumin. On the right: comparison of adhering SRGF ASC after perfusion at 0.25 dyn/cm^2 on collagen type I or on uncoated chamber slide; (D) reference curve describing dependence of adherent SRGF ASC number from flowing ASC shear stress at the concentration of 100 cells/µL. The density of adherent cells on HT1080 after perfusion at 0.1 dyn/cm^2 was extremely high (data not shown) suggesting upper saturation limit of the system was reached. SRGF ASC perfusions were performed at different flow rates in standard flow medium, i.e., 10% FBS α-MEM medium added with 2% bovine serum albumin. *, P<0.01 versus "Uncoated". c/mm^2, cells/mm^2; c/µL, cells/µL.

in *Figure 1D*, to setup experimental conditions, we defined a reference curve correlating shear stress and density of post-perfusion adherent SRGF ASC on HT1080 cancer cells. In such preliminary experiments, concentration of flowing SRGF ASC on HT1080 cells was kept at 100 cells/µL. Perfusion at 0.1 dyn/cm^2 provided an extremely high adhesion level (data not shown) suggesting upper saturation limit of the system was reached. Linear regression line was analyzed considering only adherent ASC number at 0.25, 0.5 and 0.75 dyn/cm^2. At higher shear rate (1.25 dyn/cm^2) the number of adherent cells was markedly out of linearity. Experimental perfusions on HT1080 and T98G were performed at 0.25 and 0.5 dyn/cm^2. Considering obtained results, perfusions on Huh7 were performed at 0.25 dyn/cm^2 but not at 0.5 dyn/cm^2.

Calcium signaling in static conditions

In this work, we compared the capacity of FBS and SRGF ASC to dynamically change intracellular calcium concentrations as response to extracellular stimuli. To reach this aim, we analyzed, in static conditions, kinetics of intracellular calcium concentration changes triggered by cell exposure to the calcium ionophore A23187 (Sigma). ASC were seeded at 5.0×10^3 cells/well in uncoated 24 well plate (BD) and cells were left to adhere overnight. ASC were labeled by incubation for 20 minutes at 37 °C with 8 µM Fluo 4-AM (Molecular probes – ThermoFisher). After a double cell wash with PBS, fresh medium was replaced and cells were put in the incubator for 30 minutes. The 24 well-plate was placed on an inverted fluorescence microscope equipped with a bandpass filter 480/520 and with a high sensitivity digital camera (Nikon DS, Nikon). Programmed acquisition of 1 image/3 seconds (3 minutes) of green Fluo 4-AM labeled cells was started (NIS-Elements, Nikon). Five seconds after image acquisition program was started, complete 10% FBS or 5% SRGF α-MEM medium containing 2 mM $CaCl_2$ and 5 M A23187 ionophore was added. Intracellular fluorescence changes were analyzed by an image processing software (Fiji Is Just ImageJ, NIH, MA, USA) (23). Modal background values were subtracted in each image using the "Math, Subtract" function. Regions of interest were manually traced around selected cells. Image threshold was adjusted by default automated parameters (with little adjustment, when needed). Images were then analyzed by the "Measure" function and mean fluorescence values were analyzed in each region of interest, within each image.

Calcium signaling in dynamic conditions

To assess SRGF ASC calcium signaling response after cell adhesion in dynamic conditions, we perfused 8 µM Fluo 4-AM labeled SRGF ASC in fibronectin and collagen type I coated parallel flow chamber slides (0.1 dyn/cm^2). In parallel, Fluo 4-AM labeled SRGF ASC were also perfused onto subconfluent HT1080 cells in flow chamber slides (0.25 dyn/cm^2). Sequential image acquisition of adhering green fluorescent cells was performed (1 image/5 seconds for 45 minutes). Thirty minutes after image acquisition beginning, 10 mM EDTA (Sigma) was added to the flowing medium. Intracellular fluorescence changes were analyzed following abovementioned procedure.

Flow cytometry

Expression of selected markers was evaluated on ASC using the following antibodies: CD49a PE, CD49b PE, CD49c PE, CD49d PerCP-Cy5.5, CD49e PE, CD29 APC, CD54 (ICAM1) FITC, CD106 (VCAM1) PE, CD184 (CXCR4) PE, CXCL12 (SDF1) PerCP, CD11a PE. Intracellular expression of CD184 and of CXCL12 was evaluated taking advantage of the Fixation/Permeabilization Solution Kit (BD). Phenotype analysis of cancer cells and HUVEC was performed using CD54 ICAM1 FITC and CD106 VCAM1 PE antibodies. Samples were acquired on a BD FACSCanto II flow cytometer and analyzed by BD Diva software. All experiments were performed upon instrument calibration with CS&T beads (BD).

Statistics and calculations

Data are presented as mean ± SEM. Paired or unpaired Student's *t*-test was applied to compare cell adhesion on collagen type I coated versus uncoated chambers, FBS versus SRGF ASC adhesion on collagen type I, on fibronectin, on HT1080, on T98G and on Huh7. Correlation coefficients (R^2) of reference ASC adhesion curves were calculated and tested by Regression Model Analysis Test. Two way factorial Analysis of Variance (ANOVA) for independent samples with interaction, with Tukey's HSD with Bonferroni's correction as post hoc

analysis, was applied to analyze (I) the influence of medium additive and of different perfusion substrates on ASC adhesion density after perfusion at 0.25 dyn/cm^2; (II) the impact of heparin, EDTA and anti-CD49a antibody on FBS and SRGF ASC on different substrates. Percent cell detachment after the adhesion strength test was assessed subtracting to the initial 100% value, the mean of adherent cell number measured after shear stress steps at 14.21 and 17.06 dyn/cm^2. Area under the curve of fluorescence values related to intracellular calcium concentration changes in adherent ASC stimulated with calcium ionophore was calculated by Excel software (Microsoft co., Washington, USA). Height and oscillation period of intracellular calcium peaks in SRGF ASC after adhesion to the substrate in dynamic conditions were analyzed by a Matlab® customized application.

Results

Adhesion on extracellular matrix proteins in dynamic conditions

SRGF and FBS ASC were perfused at constant continuous flow into standardized parallel flow chambers (*Figures S1,1A*). Through all the experimental cell adhesion assays, mean ASC concentration in the flowing medium was 90±15 cells/μL. Results regarding ASC adhesion capacity on collagen type I and fibronectin were reported in *Figure 2*. At 0.1 dyn/cm^2 adhesion kinetics of FBS ASC on both collagen type I and fibronectin were shown to be faster, when compared to SRGF ASC (*Figure 2A*). Coherently, at the end of perfusion, final density of adherent SRGF ASC was shown to be lower versus FBS ASC, both on collagen type I and on fibronectin (*Figure 2B*). At the end of perfusion, binding stability of adherent cells was tested imposing discrete flow steps at incremental shear stress (adhesion strength test). Kinetics of SRGF and FBS ASC displacement both from collagen type I and fibronectin were not different (*Figure 2C*). At the end of the adhesion strength test, the fraction of detached FBS and SRGF ASC from both fibronectin and collagen type I was lower than –21.0%. Dynamic adhesion assays on collagen type I and fibronectin were performed also at 0.25 dyn/cm^2: at the end of constant perfusion, a lower number of adherent SRGF ASC on collagen type I was observed, when compared to FBS ASC (38.9±6.3 versus 79.5±4.0 cells/mm^2; P<0.01). After perfusions on fibronectin, the number of adherent FBS and SRGF ASC was not significantly different (36.0±8.6 and 24.2±13.4 cells/mm^2). Adhesion and detachment kinetics of FBS and SRGF ASC at 0.25 dyn/cm^2 were not assessed. During perfusions of FBS and SRGF ASC, both at 0.1 and 0.25 dyn/cm^2, a negligible number of cells rolling events could be observed (data not shown).

Molecular characterization of FBS and SRGF ASC interaction with the extracellular matrix

In order to characterize types of receptors mediating cell adhesion, microfluidic assays at 0.1 dyn/cm^2 were repeated incubating FBS and SRGF ASC with heparin or EDTA before perfusion. In *Figure 3*, density of adherent FBS or SRGF ASC in standard perfusion medium was considered as 100% and adhesion of FBS or SRGF ASC after addition of heparin and EDTA was expressed as percent relatively to ASC adhesion in standard medium. Heparin addition to FBS and SRGF ASC before perfusion on both collagen type I and fibronectin failed to significantly affect adherent cell density (*Figure 3A*), binding kinetics (*Figure 3B*), and cell detachment kinetics (*Figure 3C*). In particular, at the end of adhesion strength test, the mean fraction of detached FBS and SRGF ASC from fibronectin and from collagen type I was 16.2%±0.7% and 7.3%±1.1%, respectively (*Figure 3D*). Otherwise, as shown in *Figure 3A*, EDTA addition to FBS and SRGF ASC before perfusions on both substrates severely reduced the relative density of post perfusion adherent ASC. In such conditions, binding kinetics and adhesion strength test could not be measured.

As shown in *Table 1*, we evaluated by flow cytometry the expression level of selected integrins in ASC: FBS and SRGF ASC did not show differential expression of CD49b, CD49c, CD49d, CD49e as well as CD29. Otherwise, as shown in *Figure 4A*, CD49a was markedly expressed in FBS ASC only. To assay the role of CD49a as potential factor explaining the different affinity of SRGF and FBS ASC for extracellular matrix proteins, we performed microfluidic adhesion assays (0.25 dyn/cm^2) incubating, before perfusion, ASC with an anti CD49a blocking antibody. Parallel flow chambers were coated with collagen type I and fibronectin. As reported in *Figure 4B*, antibody addition inhibited binding of FBS ASC only (–54%±5% versus no antibody): the number of post-perfusion adherent FBS ASC in presence of anti CD49a was not different from adherent SRGF ASC number (with or without antibody inhibition). Presence of anti CD49a antibody (*Figure 4C* left) slowed adhesion kinetics of FBS ASC, when compared to FBS ASC perfusions without antibody; otherwise, adhesion kinetics

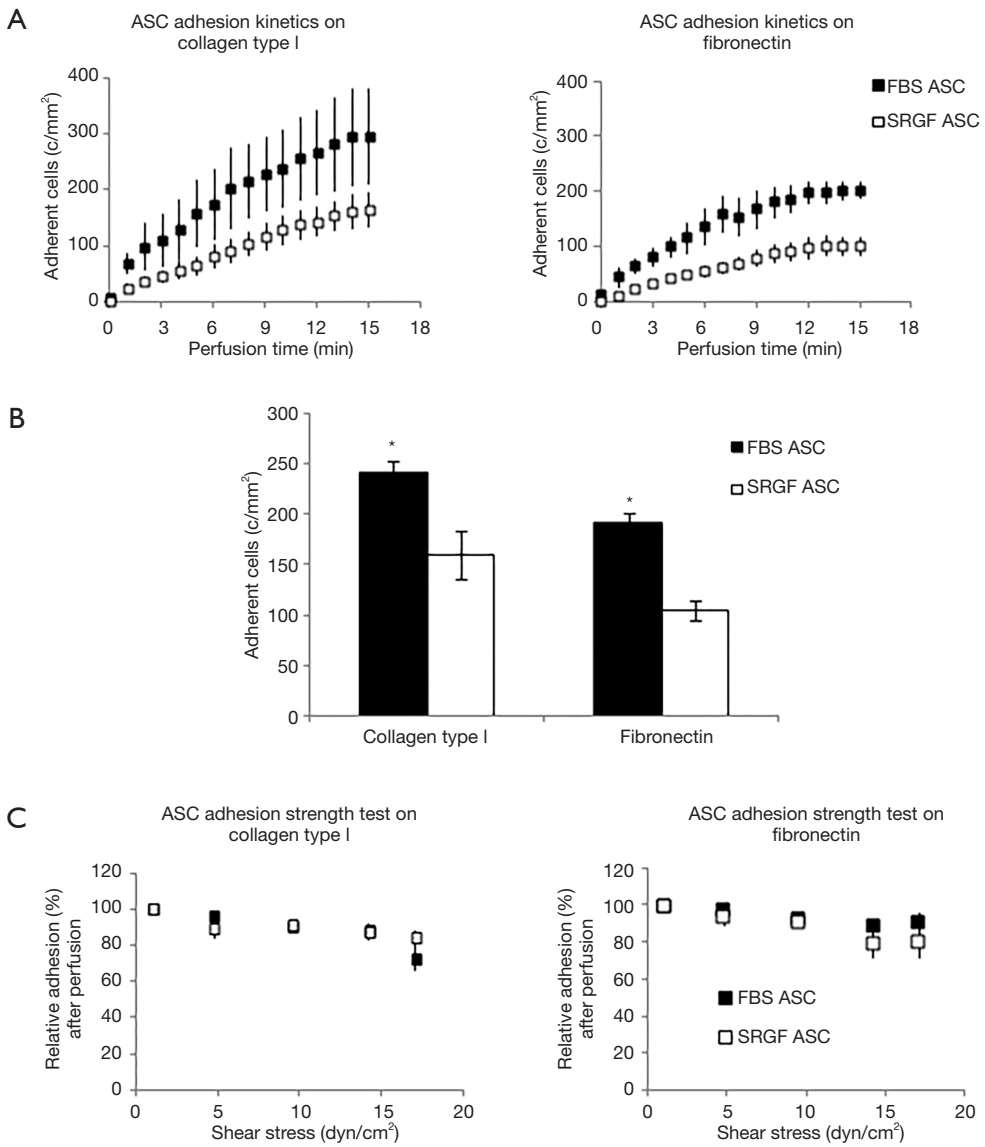

Figure 2 ASC adhesion on collagen type I and fibronectin. FBS and SRGF ASC kinetics (A), binding potential (B), as well as adhesion stability (C) on collagen type I and fibronectin. In (C) density of adherent FBS or SRGF ASC immediately after perfusion in standard medium was expressed as 100% (first dot) and the fraction of adhering FBS or SRGF ASC along with the adhesion strength test was relatively expressed as percent. Results derived from perfusions of FBS and SRGF ASC performed at 0.1 dyn/cm^2 were reported. Standard medium, 10% FBS α-MEM medium added with 2% bovine serum albumin; *, P<0.01 versus SRGF ASC; c/mm^2, cells/mm^2.

of SRGF ASC was not affected by cell incubation with the antibody (*Figure 4C* right). Nevertheless, anti CD49a blocking antibody displayed a tendency to slow kinetics of SRGF ASC (*Figure 4C* right) in early adhesion phases (from 3rd to 9th minute of perfusion). CD49a inhibition did not significantly affect the fraction of detached FBS (–16.8%±4.1%) and SRGF ASC (–19.1%±4.8%) after adhesion strength test (*Figure 4C* left and right).

Adhesion on HUVEC in dynamic conditions

Affinity of SRGF and FBS ASC for endothelial cells was tested by microfluidic adhesion assays in which HUVEC were cultured for 12–18 hours in a sterile

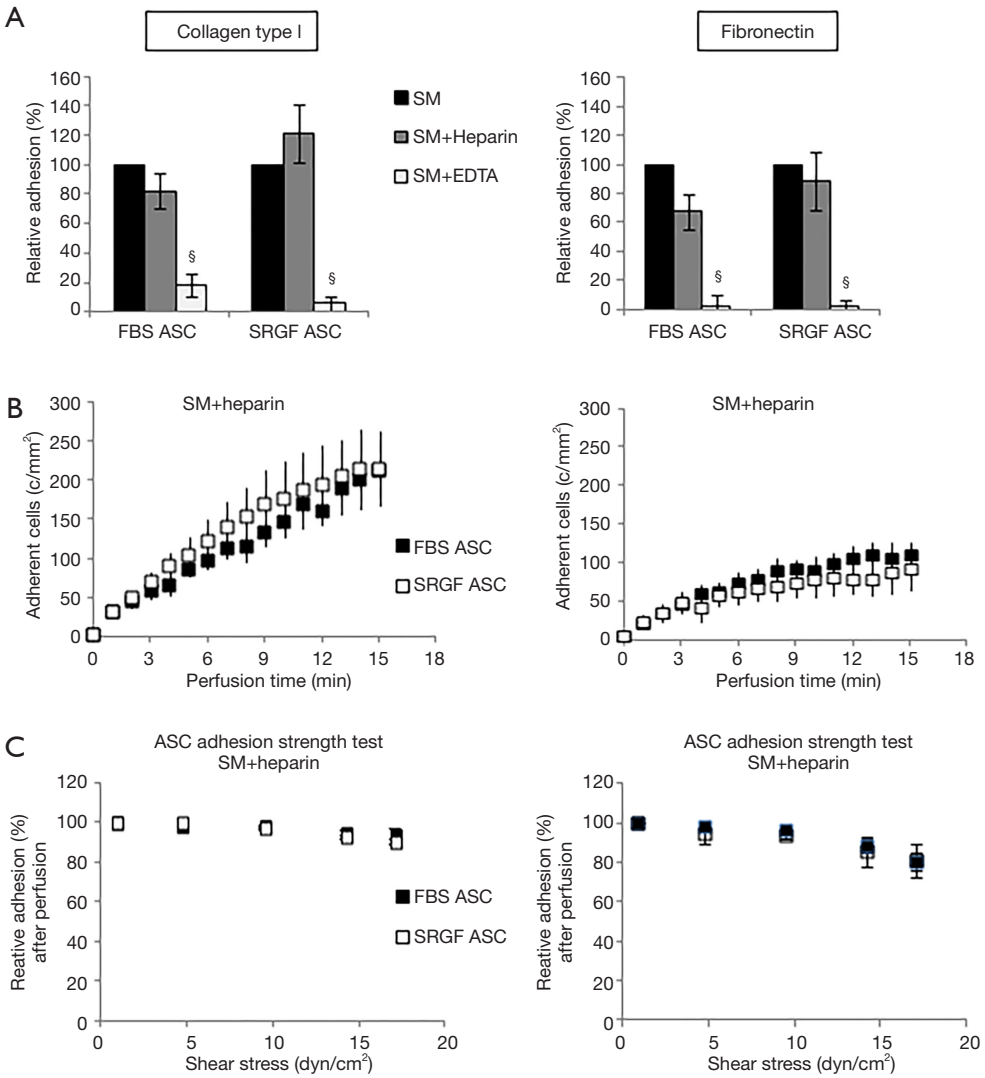

Figure 3 Impact of heparin and EDTA on ASC adhesion on collagen type I and fibronectin. Impact of heparin and EDTA on FBS and SRGF ASC binding potential (A), kinetics (B) as well as adhesion stability (C) on collagen type I and fibronectin. In (A) density of adherent FBS (248±20 cells/mm^2 on collagen type I and 191±15 cells/mm^2 on fibronectin) or SRGF (160±24 cells/mm^2 on collagen type I and 104±10 cells/mm^2 on fibronectin) ASC adhesion in SM (*Figure 2B*) was considered as 100%; adhesion of FBS or SRGF ASC after addition of heparin and EDTA was expressed as percent (%) relatively to ASC adhesion in SM. In (C) density of adherent FBS or SRGF ASC immediately after perfusion in heparin added SM was expressed as 100% (first dot) and the fraction of adhering FBS or SRGF ASC along with the adhesion strength test was relatively expressed as percent. FBS and SRGF ASC perfusions were performed at 0.1 dyn/cm^2. §, P<0.1 versus SM. SM, standard medium i.e., 10% FBS α-MEM medium added with 2% bovine serum albumin; c/mm^2, cells/mm^2.

chamber at 37 ℃. FBS and SRGF ASC were perfused at 0.1 dyn/cm^2 in the same chamber slide with or without addition of TNF-α. As shown in *Figure 5A*, the density of adhering FBS and SRGF ASC was markedly higher when HUVEC cells were treated with TNF-α. When compared to SRGF ASC, a higher number of FBS ASC was shown to adhere to TNF-α treated HUVEC cells. Otherwise, the number of SRGF and FBS ASC adhering to untreated HUVEC was not significantly different. HUVEC incubation with TNF-α induced an FBS and SRGF ASC adhesion increase of 5.0±0.1 and 5.1±0.2 folds (*Figure 5A*). As shown in *Figure 5B*, HUVEC exposure to

Table 1 Expression levels of cell adhesion molecules in FBS and SRGF ASC

Cell adhesion molecules	FBS ASC	SRGF ASC
Integrins		
CD49b	+	+
CD49c	+	+
CD49d	+/–	+/–
CD49e	++	++
CD29	++	++
Cell-cell interaction molecules		
CD54 ICAM1	–	–
CD106 VCAM1	–	–
CD11a	–	–
CD184 CXCR4 (extracellular)	–	–
CXCL12 SDF1 (extracellular)	–	–
CD184 CXCR4 (intracellular)	+/–	+/–
CXCL12 SDF1 (intracellular)	–	–

++, bright expression; +, positive expression; +/–, dim expression.

TNF-α increased the expression of CD54 ICAM1; similarly, CD106 VCAM1 expression was upregulated by TNF-α in a subpopulation of HUVEC cells.

Adhesion on cancer cells in dynamic conditions

In this work we also tested the ability of FBS and SRGF ASC to directly adhere at 0.25 dyn/cm^2 on three different cancer cell lines, HT1080, T98G and Huh7. As displayed in *Figure 6A*, after perfusion, the number of adherent SRGF ASC on both HT1080 and T98G cells was higher than FBS ASC. Coherently, adhesion kinetics (*Figure 6B*) of SRGF ASC on both HT1080 and T98G cells was faster than FBS ASC. Kinetics of SRGF and FBS ASC displacement from both HT1080 and T98G (adhesion strength test) was not significantly different (*Figure 6B*). The large majority of both FBS and SRGF ASC (–96.0% to –100%) detached from cancer cells after high shear stress steps (*Figure 6A*). Noteworthy, the number of both FBS and SRGF ASC adhering onto Huh7 cells was negligible (*Figure 6A*): kinetics of ASC adhesion and displacement was not evaluated on Huh7. Additional ASC adhesion assays in microfluidic conditions were performed at 0.5 dyn/cm^2 on HT1080 and T98G. After perfusion the number of adherent SRGF ASC (25.2±4.5 cells/mm^2) on HT1080 was significantly ($P<0.01$) higher than FBS ASC (1.8±0.8 cells/mm^2). Similarly, adherent SRGF ASC density (24.4±4.5) on T98G was significantly ($P<0.01$) higher than FBS ASC (0.5±0.1). Perfusions at 0.5 dyn/cm^2 were not performed on Huh7. Representative images of fluorescently labeled ASC interacting with cancer cells were reported in *Figure 6C*. Analyzing together the density of adhering FBS and SRGF ASC after perfusion at 0.25 dyn/cm^2 on relevant substrates as fibronectin, collagen type I, HT1080, T98G and Huh7 we could demonstrate that medium additives played a significant role ($P<0.01$) while substrates only tended ($P=0.06$) to affect ASC adhesion. Medium additives and substrates significantly interacted ($P<0.05$) to modify density of adhering ASC in microfluidic conditions. Post hoc analysis confirmed that, in such flow conditions, cell culture medium significantly ($P<0.05$) affected ASC adhesion only on collagen type I, as well as on HT1080 and T98G cells.

Characterization of FBS and SRGF ASC interaction with cancer cells

As reported by flow cytometry results in *Figure 6D*, CD54 ICAM1 was not expressed in both HT1080 and T98G cells, while it was markedly expressed in Huh7 cells. CD106 VCAM1 was not expressed in HT1080 and Huh7, while it was partially expressed by T98G cells. *Figure* 7 shows the impact of heparin and EDTA on FBS and SRGF ASC adhesion on HT1080 (a) and T98G (b): the number of adherent FBS and SRGF ASC after perfusion in standard medium on both cellular substrates was defined as 100%. ANOVA analysis showed that, in presence of heparin, when compared to FBS ASC, a higher number of SRGF ASC adhered to both HT1080 and T98G after perfusion (*Figure 7A,B*). Still, in presence of heparin, a lower number of FBS ASC, but not of SRGF ASC, adhered on both HT1080 and T98G versus standard medium (*Figure 7A,B*). In presence of EDTA, the number of adherent SRGF ASC was higher than FBS ASC only when cells were perfused on HT1080 (*Figure 7A*), i.e., not on T98G. Moreover, on both HT1080 and T98G, when compared to perfusions in standard medium, the number of adherent SRGF ASC was not affected by EDTA (*Figure 7A,B*). Otherwise, the number of adherent FBS ASC was reduced in presence of EDTA versus standard medium, only when cells were perfused on HT1080, i.e., not on T98G (*Figure 7A*). When compared

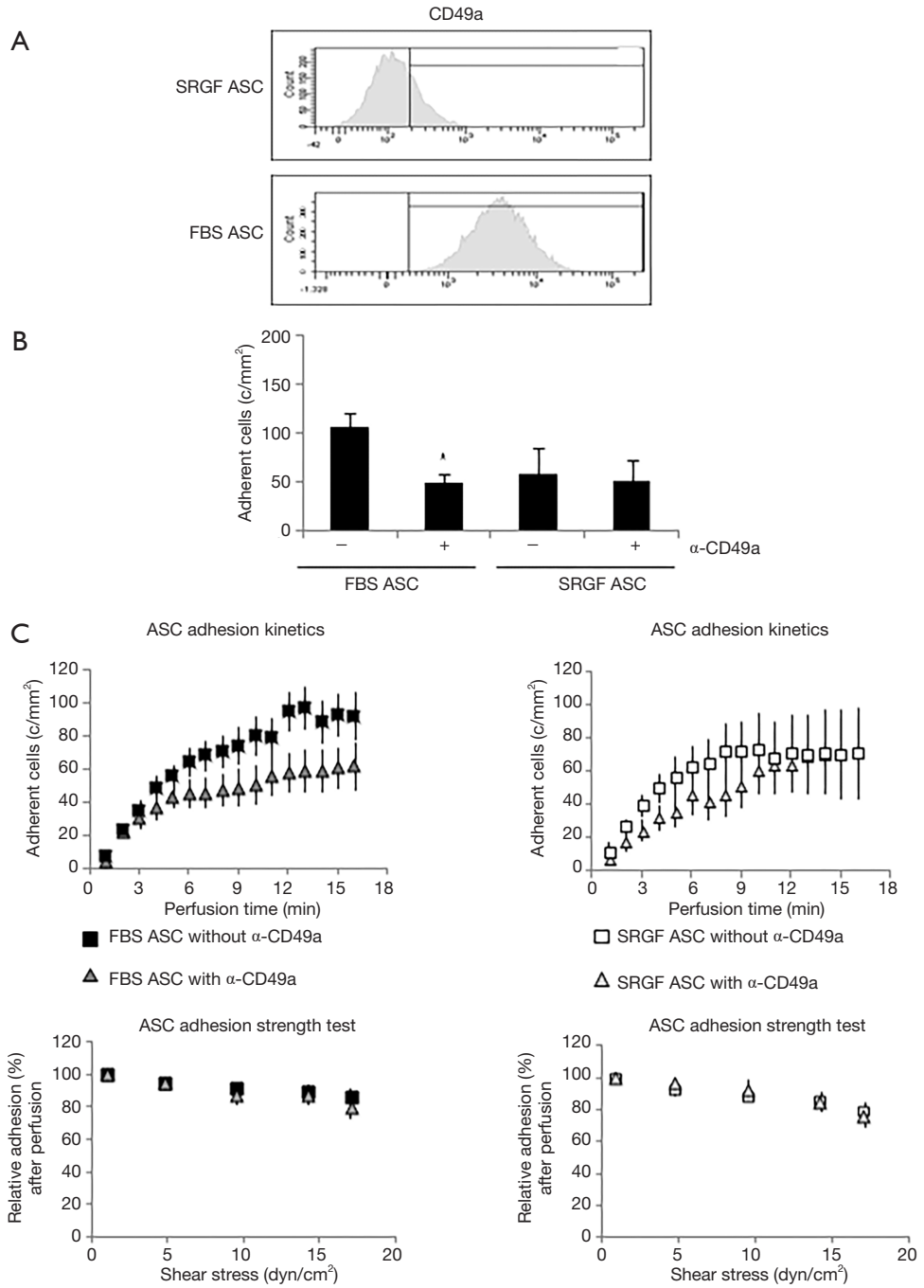

Figure 4 Role of CD49a in FBS and SRGF ASC adhesion on collagen type I and fibronectin. (A) Representative example of CD49a expression analysis performed by flow cytometry in FBS and SRGF ASC. The threshold discriminating positively labeled cells was defined analyzing FBS or SRGF ASC in presence of the appropriate isotype control antibody (histogram not shown); (B) effect of anti-CD49a blocking antibody on FBS and SRGF ASC binding potential on collagen type I and fibronectin; (C) effect of anti-CD49a blocking antibody on FBS and SRGF ASC binding kinetics and adhesion stability on collagen type I and fibronectin. In ASC adhesion strength test reported in (C), density of adherent FBS or SRGF ASC immediately after perfusion in anti-CD49a added SM was expressed as 100% (first dot) and the fraction of adhering FBS or SRGF ASC along with the adhesion strength test was relatively expressed as percent. Assessments of CD49a expression (A) and function (B) were performed in FBS and SRGF ASC derived from all 5 patients. Perfusions were performed at 0.25 dyn/cm^2 in standard medium (10% FBS α-MEM medium added with 2% bovine serum albumin); c/mm^2, cells/mm^2.

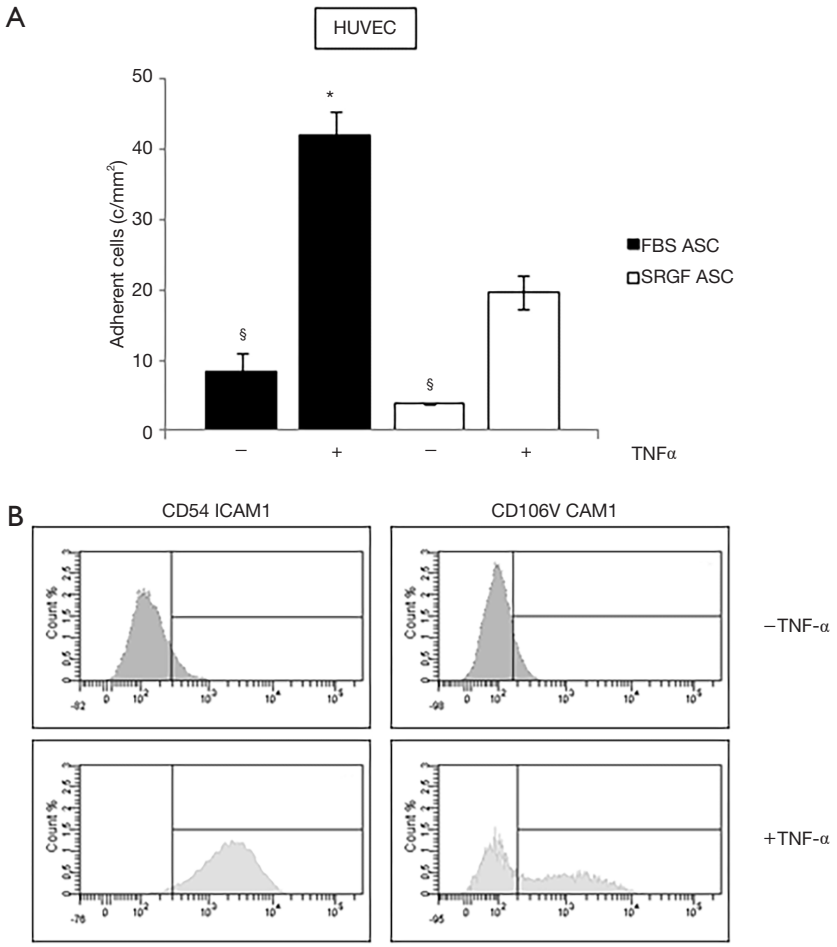

Figure 5 FBS and SRGF ASC affinity for HUVEC cells. (A) Analysis of FBS and SRGF ASC affinity in dynamic flow conditions for HUVEC cells with and without exposure to TNF-α. Perfusions were performed at 0.1 dyn/cm^2 in standard medium (10% FBS α-MEM medium added with 2% bovine serum albumin); (B) expression of CD54 ICAM1 and CD106 VCAM1 in HUVEC cells with and without exposure to TNF-α, analyzed by flow cytometry. The threshold discriminating positively labeled cells was defined analyzing FBS or SRGF ASC in presence of the appropriate isotype control antibody (histogram not shown). c/mm^2, cells/mm^2.

to FBS ASC, SRGF ASC adhesion kinetics on HT1080 was faster in presence of both heparin and EDTA (*Figure 7C*). On T98G, SRGF ASC adhesion kinetics was faster than FBS ASC only in presence of heparin (*Figure 7D*). Displacement kinetics of FBS and SRGF ASC (adhesion strength test) from both HT1080 and T98G was not different either in presence of heparin or EDTA (*Figure 7C,D*). In presence of heparin and of EDTA, the large majority of FBS and SRGF ASC (from –95.0% to –99%) detached from cancer cells after high shear stress steps. Expression of selected receptors and ligands involved in cell-cell interaction was assessed in both FBS and SRGF ASC by flow cytometry. Results are reported in *Table 1*.

Analysis of FBS and SRGF ASC response to extracellular stimuli

The capacity of FBS and SRGF ASC to react to an external stimulus as the administration of a calcium ionophore, was reported in *Figure 8A*. As demonstrated by fluorescence quantification in Fluo 4-AM labeled cells, administration of A23187 at equal concentrations induced markedly higher intracellular calcium concentration changes over time in SRGF ASC (AUC ratio: 1,97±0.2) when compared to FBS ASC. Calcium movements triggered by A23187 in FBS ASC were almost negligible (*Figure 8A*). In both FBS and SRGF ASC, fluorescence changes were not observed in

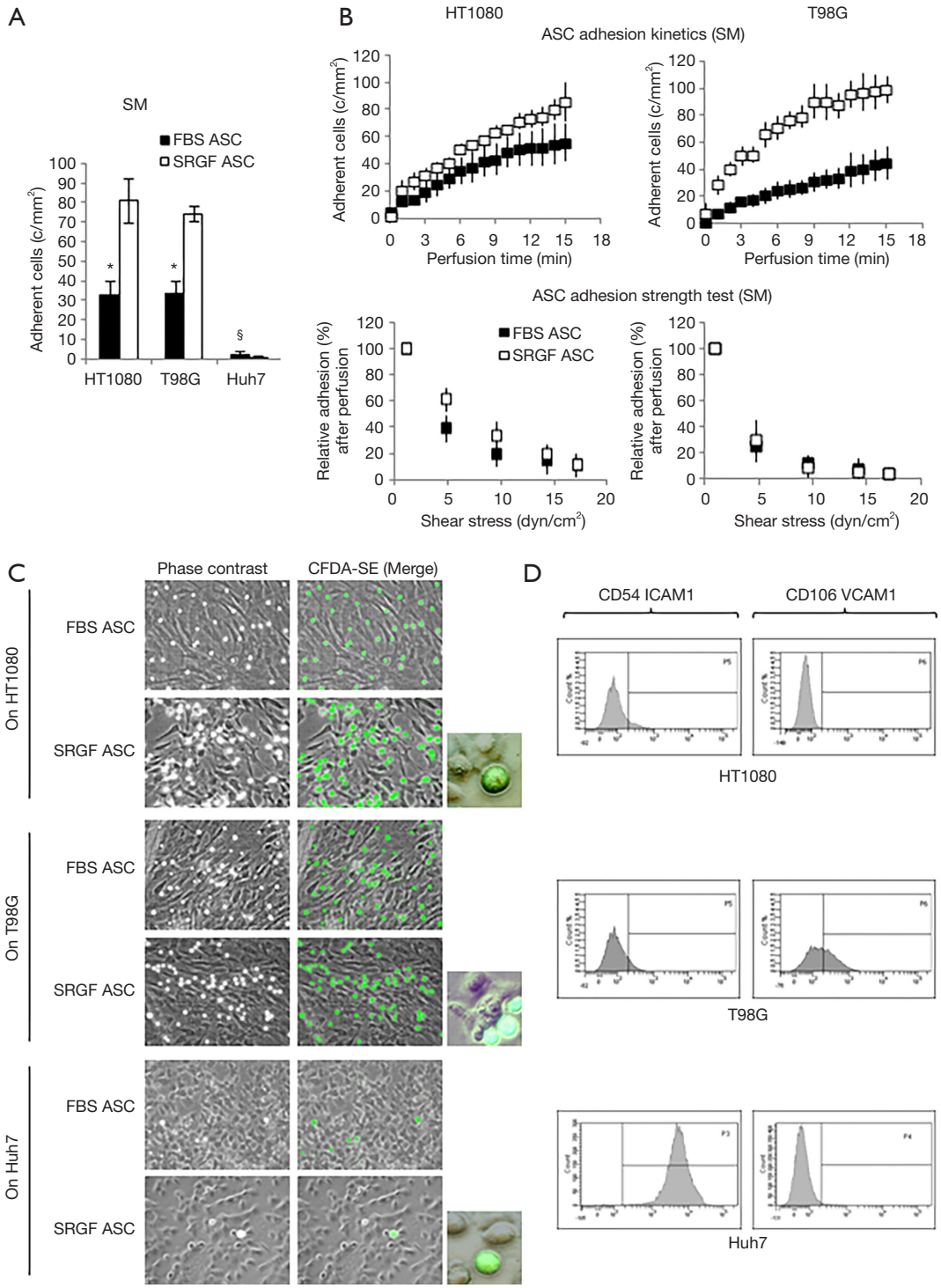

Figure 6 ASC adhesion on HT1080, T98G and Huh7. Analysis of FBS and SRGF binding potential (A), kinetics as well as adhesion stability (B) in dynamic flow conditions for HT1080, T98G and Huh7. In ASC adhesion strength test reported in (B), density of adherent FBS or SRGF ASC immediately after perfusion SM was expressed as 100% (first dot) and the fraction of adhering FBS or SRGF ASC along with the adhesion strength test was relatively expressed as percent. Perfusions were performed at 0.25 dyn/cm^2; (C) representative images of fluorescently labeled FBS and SRGF ASC interacting with cancer cells after perfusions in the flow chamber. Perfusions were performed at 0.25 dyn/cm^2; (D) expression of CD54 ICAM1 and CD106 VCAM1 in cancer cells analyzed by flow cytometry. SM, standard medium i.e., 10% FBS α-MEM medium added with 2% bovine serum albumin; *, P<0.01 versus SRGF ASC; §, P<0.01 versus HT1080 and T98G; c/mm^2, cells/mm^2.

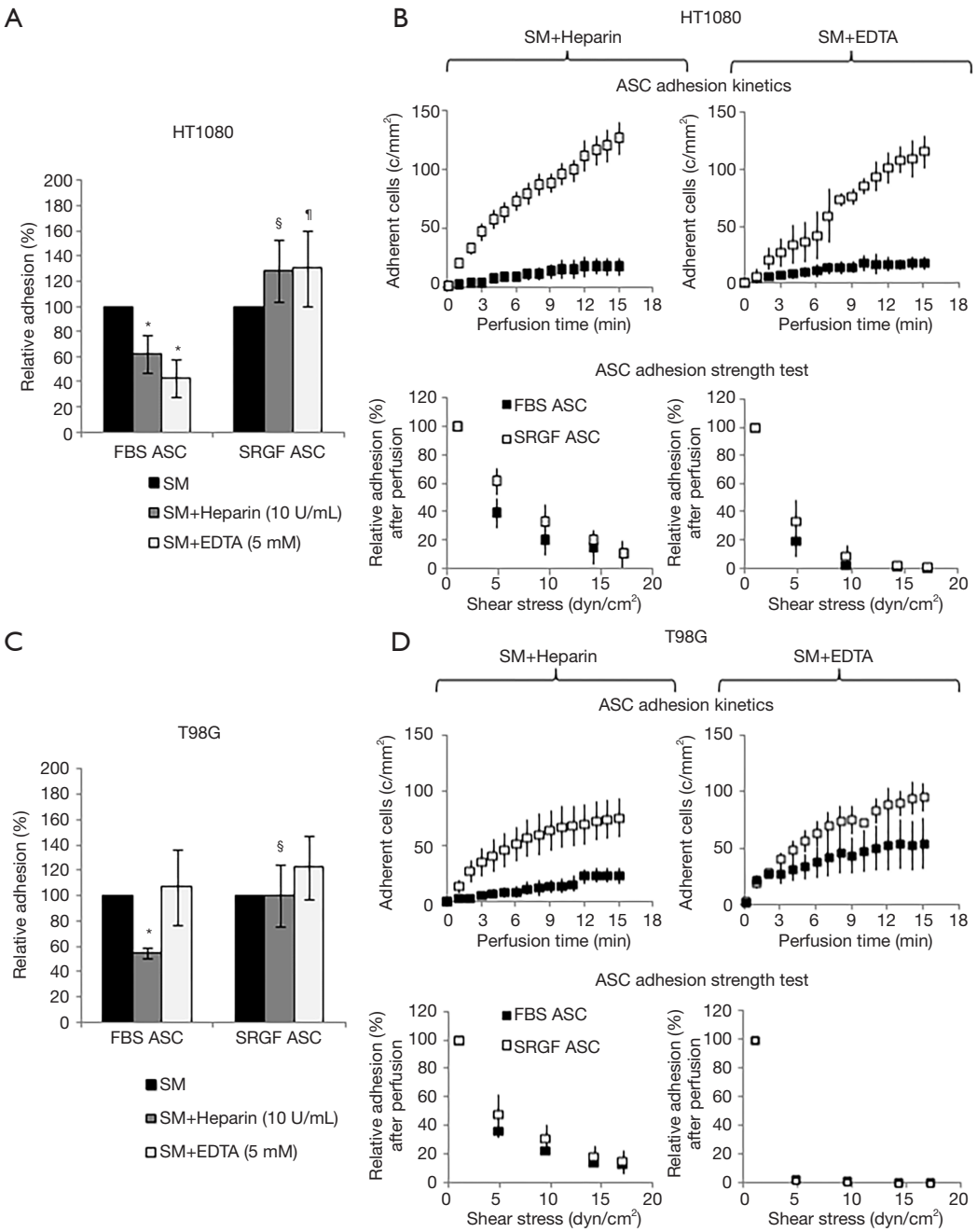

Figure 7 Impact of heparin and EDTA on ASC adhesion on HT1080, T98G and Huh7. The impact of heparin and EDTA on FBS and SRGF ASC binding potential on HT1080 (A) and T98G (B): the number of adherent FBS (32±7 cells/mm^2 on HT1080 and 34±6 cells/mm^2 on T98G) and SRGF (81±11 cells/mm^2 on HT1080 and 74±4 cells/mm^2 on T98G) ASC after perfusion in standard medium on both cellular substrates (*Figure 6A*) was defined as 100%; adhesion of FBS or SRGF ASC after addition of heparin and EDTA was expressed as percent (%) relatively to ASC adhesion in SM. Moreover, *Figure* 7 displays the impact of heparin and EDTA on FBS and SRGF ASC kinetics as well as adhesion stability on HT1080 (C) and T98G (D). In ASC adhesion strength test reported in (C) and (D), density of adherent FBS or SRGF ASC immediately after perfusion in heparin or EDTA added SM was expressed as 100% (first dot) and the fraction of adhering FBS or SRGF ASC along with the adhesion strength test was relatively expressed as percent. *, P<0.05 versus FBS ASC perfused in SM; §, P<0.05 *vs.* FBS ASC perfused in SM + Heparin; ¶, P<0.01 *vs.* FBS ASC perfused in SM + EDTA; SM, standard medium (10% FBS α-MEM medium added with 2% bovine serum albumin); c/mm^2, cells/mm^2.

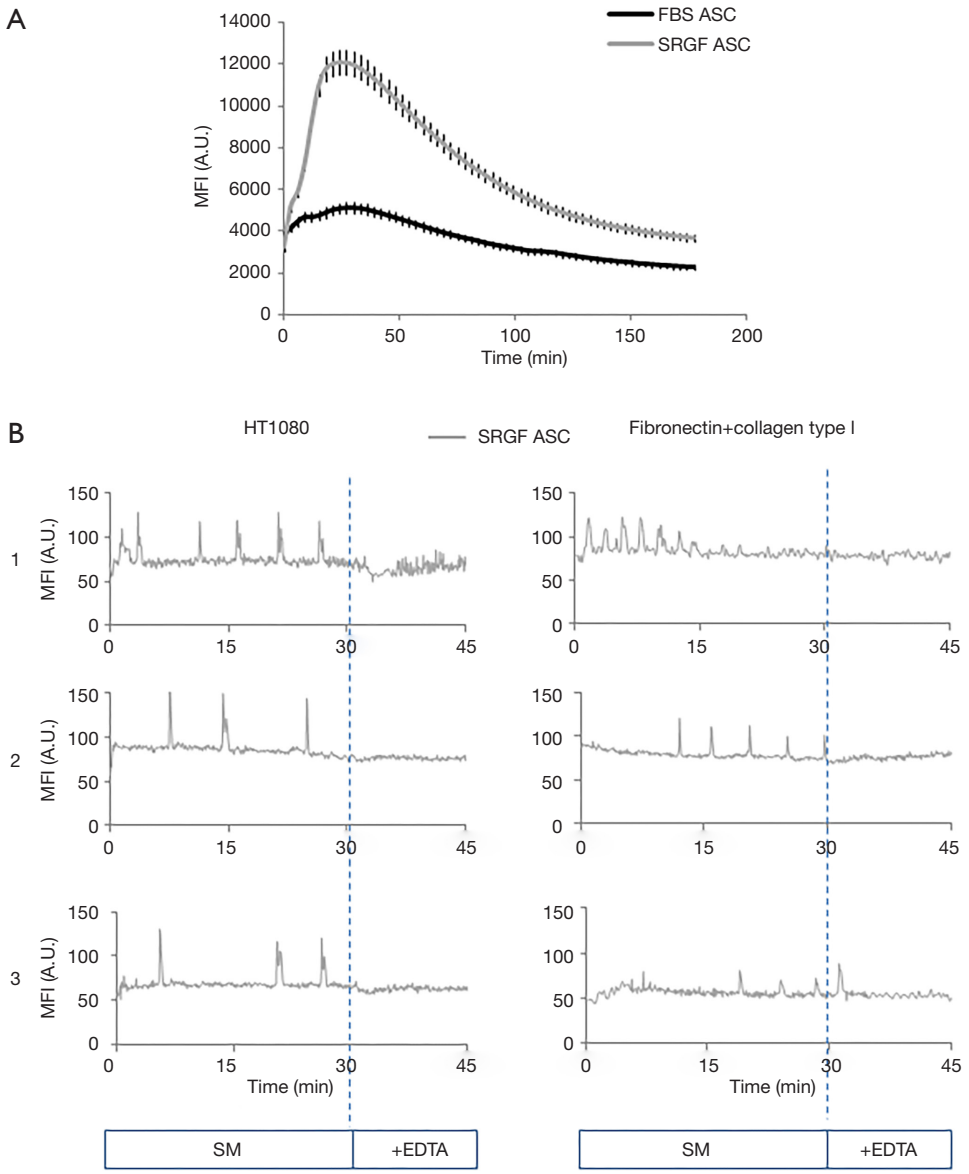

Figure 8 Intracellular concentration changes in FBS and SRGF ASC. (A) Changes over time of intracellular mean fluorescence intensity in FBS and SRGF ASC in static conditions. Cells were labeled with Fluo 4-AM calcium specific dye. Calcium mobilization was triggered by addition to the cell culture medium of the A23187 ionophore; (B) changes over time of intracellular mean fluorescence intensity in SRGF ASC labeled by Fluo 4-AM dye. Three representative graphs [1-3] describing single cell fluorescence changes over time after SRGF ASC adhesion on HT1080 or extracellular matrix were reported. Cell fluorescence analysis was performed in at least 50 single SRGF ASC derived from all 5 patients. In (B), cells were not stimulated by the ionophore. Sequential images were acquired of labeled SRGF ASC immediately after adhesion in parallel flow chambers on HT1080 (0.25 dyn/cm^2) or on fibronectin and collagen type I (0.1 dyn/cm^2). After 30 minutes perfusion in standard medium i.e., 10% FBS α-MEM medium added with 2% bovine serum albumin, EDTA was added for the remaining 15 minutes. MFI, mean fluorescence intensity; A.U., arbitrary units.

absence of $CaCl_2$ in culture medium (data not shown).

Fluo 4-AM labeled SRGF ASC were perfused on HT1080 and on collagen type I and fibronectin coated surfaces: quantification of cell fluorescence changes over time demonstrated that such cells can activate a rhythmic intracellular response after adhesion of both cellular and protein substrates (*Figure 8B*). After adhesion on fibronectin and collagen type I, calcium peak train duration was 20.7±1.9 min, peak period was 2.7±1.3 min and mean peak height (from baseline) was 34±8 arbitrary units of fluorescence intensity. Similarly, after adhesion on HT1080, calcium peak train duration was 14.8±0.7 s, peak period was 3.1±1.2 min and mean peak height (from baseline) was 52±9 arbitrary units of fluorescence intensity. Addition of EDTA (30 minutes after perfusion beginning) blunted rhythmic intracellular calcium concentration changes in all analyzed conditions (*Figure 8B*).

Conclusions

Circulating ASC, as well as MSC from other tissues, are characterized by a tropism for cancers cells *in vivo*, whose mechanisms are still not completely characterized (7,11,25,26). ASC can extravasate by transendothelial migration after tethering and coordinated rolling on vascular endothelium; thereafter, they can reach the tumor mass by active migration (11,12). In order to comply with GMP guidelines, *ex vivo* ASC expansion for clinical applications must be performed using growth factors of human origin (27). These active substances are available in our SRGF product, and we previously demonstrated that such medium additive can increase ASC expansion rate without inducing cell transformation or altering cell differentiation potential even after extended population doublings (2). In this work, we investigated the impact of SRGF on ASC capacity to adhere on selected extracellular matrix proteins or on cancer cells in dynamic conditions, as marker of ASC homing potential. We took advantage of ASC derived from SVF isolated from breast cancer patients, considering the intended use for potential future applications. The autologous setting is, in fact, preferred when repeated cell infusions to the same patient are required as e.g., for drug delivery applications. Moreover, both FBS and SRGF ASC were expanded in parallel from each enclosed patient: thus, we can exclude the comparison between such cells to be biased by the underlying pathology. Despite strong interindividual variability, SVF from breast cancer patients previously showed mildly increased self renewal and potentially inhibited differentiation capacity due to cell microenvironmental modifications mediated by drug therapy or by the tumor itself (28). Conditioning of progenitor cells within the organism can be overcome by *ex vivo* ASC expansion: cultured ASC are, in fact, characterized by better homogeneity and such cells showed consistently improved clinical results in regenerative and reconstructive medicine (29). As previously shown, we used FBS and SRGF ASC within growth phases in which proliferation rate, phenotype, potency and karyotype were stable (2). Considering their enhanced proliferation potential (2) we used SRGF ASC until a higher level of population doublings in order to perform a comparison with FBS ASC in paired conditions. We took advantage of a microfluidic *in vitro* model in which ASC were directly perfused on extracellular matrix proteins or on cancer cells: this would represent a model limitation as extravasation and migration toward cancer cells (11) are not considered. Nevertheless, published data demonstrated that cancer vessel is characterized by frequent discontinuity of the endothelium, thus allowing direct contact between blood and tumor cells (30). So, our experimental model overcomes static experimental setting and it allows a reliable analysis of ASC adhesion capacity. Appropriate experimental shear stress was empirically determined within the range of *in vivo* rheological conditions: shear stress of interstitial flow in cancer tissue or in sinusoids and small veins was reported to be approximately of 0.1–0.5 dyn/cm^2 (31). At low shear stress, MSC were previously shown to firmly adhere, by mean of specific integrins, on extracellular matrix proteins including fibronectin (32) and collagens (24,32). Such proteins are expressed in several organs and tissues (33): thus, in our model, ASC adhesion on such substrates was considered as not specifically directed to cancer targets. Noteworthy, our results demonstrated that addition of 5% SRGF in cell culture medium reduced off-target binding of expanded ASC. A previous work (34) demonstrated that expanding MSC in presence of human serum reduced affinity of such cells for extracellular matrix proteins. FBS and SRGF ASC adhesion on both substrates was shown to be stable because high shear stress flow imposed on interacting cells (adhesion strength test) mildly reduced the fraction of adhering cells. Direct assessment of molecular mechanisms playing such role in ASC was not performed, but previous publications showed that leukocyte adhesion is stabilized by increased expression of selected integrins (35-37). SRGF and FBS capacity to adhere on collagen type I and fibronectin was also tested in presence of heparin

and EDTA. Inhibiting P-selectin interaction with its ligand (38), heparin can prevent cell tethering and rolling on immobilized endothelial cells (39). Bone marrow derived MSC were shown not to express endothelial P-selectin ligands (12). We previously (2) demonstrated that both FBS and SRGF ASC express the E-selectin ligand CD44 (40). Our results confirm that P-selectin ligands are not involved in SRGF or FBS ASC binding on both collagen type I and fibronectin. The capacity of integrins to interact with their ligands is dependent on availability of calcium ions (41). Results obtained after EDTA addition in the cell perfusion medium suggest calcium dependent integrins to be involved in cell binding on such substrates. Analysis of selected integrins showed that CD49a was expressed in FBS ASC only. CD49a expression was previously shown to be not affected by the expansion process in MSC (42): thus, we are confident that observed CD49a regulation is mediated by the medium additive itself and not by different cell population doubling level between SRGF and FBS ASC. Experimental inhibition of CD49a reduced FBS ASC adhesion on both collagen type I and fibronectin. CD49a is known to mediate cell binding to collagen type I (43); nevertheless, we can hypothesize that in microfluidic conditions CD49a could play a role in FBS ASC binding also to fibronectin. Previous reports demonstrated that, when compared to static conditions, dynamic cell-cell interaction can involve different receptors and ligands (44). In addition, considering adhesion strength test results in presence of the blocking antibody, CD49a is not involved in stabilization of cell adhesion. Addition of CD49a blocking antibody showed a tendency to inhibit stable adhesion kinetics in the early phases of SRGF ASC perfusions: we can speculate that inhibition of the residual CD49a expression in SRGF ASC could modulate receptor mediated processes of cell capture before stable adhesion. Experimental evidence suggests that, in later adhesion kinetics phases, other receptor-ligand interactions can rescue the mild inhibitory effect mediated by CD49a blocking antibody in SRGF ASC.

We also investigated ASC capacity to adhere in fluidic conditions on expanded cells seeded into the parallel flow chamber. As abovementioned, firm adhesion on vascular endothelium is required to let MSC reach neighboring cancer cells (11). Rüster and colleagues (12) showed that bone marrow derived MSC can interact with activated endothelial cells at low shear stress (0.1 dyn/cm^2). In this work, we confirmed that our SRGF and FBS ASC can firmly adhere at low shear stress on HUVEC cells exposed of TNF-α, through upregulation of CD106 VCAM1 and CD54 ICAM1 (12). Such assay was performed to demonstrate that behavior of our ASC in dynamic conditions was comparable with previous observations. FBS ASC adhesion on activated endothelial cells was higher than SRGF ASC, but fold change relatively to not-activated endothelium was not affected by the medium additive. In a previous work (34), authors showed that MSC expanded in presence of human serum reduced cell adhesion on activated endothelial cells. Afterwards, we analyzed ASC binding onto cancer cells in microfluidic conditions and we clearly demonstrated that both FBS and SRGF ASC were not captured by hepatocarcinoma Huh7 cells. Previous publication showed that MSC from bone marrow can home to hepatocarcinoma cancer cells in a murine model (7). In such work (7) a different cell line was used for cancer induction in mice and active *in vivo* migration could be involved in observed cell homing to target sites. Interestingly, we showed that SRGF can improve specific on-target adhesion of ASC on both HT1080 and T98G cells. While previous publications showed lowered MSC homing potential after growth in cell culture (42,45), our extensively expanded SRGF ASC showed enhanced adhesion on cancer cells; thus, such effect appears to be directly related to the medium additive itself. Moreover, enhanced adhesion on cancer cells was shown to be specifically related to the tumor type as ASC, and especially SRGF ASC, were characterized by marked affinity for cell lines derived from mesenchymal cancers as sarcoma (46) and glioblastoma (47) but not for epithelial tumors as hepatocarcinoma (48).

When compared to ASC adhering to extracellular matrix proteins, the lower overall ASC binding stability on cancer cells suggests different receptors and ligands to be involved in adhesion on such substrates. Even though actual molecular mechanisms were not defined, high affinity adhesion of SRGF ASC on HT1080 and T98G was independent from selectin receptors or from calcium dependent integrins. Otherwise, our data suggest that in fluidic conditions FBS ASC adhesion on cancer cells can be modulated by selectin receptors or by calcium dependent integrins. Such integrins are not likely to be involved in stabilization of FBS and SRGF ASC adhesion on tumor cells.

Our comparative expression analysis of cell-cell interaction molecules failed to identify factors determining different avidity of FBS and SRGF ASC for cancer cells. We previously demonstrated (2) that expression of other receptors mediating cell adhesion as CD90 (49), CD44 (50),

CD166 (51), CD146 (31), CD11b (52), CD11c (53) are not differentially regulated in FBS and SRGF ASC. In addition, in our experimental conditions, expanded FBS and SRGF ASC lacked expression of CD106 VCAM1 and CD54 ICAM1. Negative or weak expression of CD106 VCAM1 was previously reported in expanded ASC (54) and variable expression of CD54 ICAM1 was demonstrated in MSC and ASC (55-57). Moreover, our results suggest, that expression of CD106 VCAM1 and CD54 ICAM1 on cancer cells is not involved in ASC adhesion on cellular substrates; their expression, in fact, is not correlated with ASC adhesion affinity for such cells seeded in the parallel flow chamber. Noteworthy, extremely low affinity cells as Huh7 were shown to positively express CD54 ICAM1. Previous works (58) reported that MSC exposure to TNF-α can upregulate cell adhesion molecules as CD106 VCAM1 and CD54 ICAM1, in turn possibly ameliorating ASC binding potential in flow conditions, but such investigation is beyond scopes of the present work.

We previously demonstrated that SRGF can induce faster ASC proliferation when compared to FBS (2). This could in principle affect cell capacity to differently mobilize intracellular calcium as response to an extracellular stimulus (59,60). We here demonstrated that only SRGF ASC can strongly mobilize calcium ions from intracellular storages when exposed to an ionophore. In turn, we showed that repeated calcium oscillation waves occurred in SRGF ASC upon adhesion. Frequency modulation of such oscillatory signaling response is known to activate specific biological responses as degranulation, secretion of active substances and exocytosis (61-63). MSC from different tissues were shown to release extracellular vesicles with therapeutic effect in several disease models (64,65) and such process was shown to be calcium dependent (66). Thus, highly proliferating SRGF ASC, in virtue of their enhanced capacity to interact (on-target) with selected cancer cells and to efficiently activate an intracellular response, could be considered as an optimal drug delivery vehicle for cancer therapy. Extensive molecular characterization of such evidence is beyond aims of this work. Further *in vivo* investigations in complex animal models shall be required to completely demonstrate advantages of SRGF ASC as cell therapy product in oncology.

Acknowledgments

We are grateful to the technical and nurse staff of the Stem cell unit of the Centro di Riferimento Oncologico di Aviano (CRO) IRCCS. We address a special thank to Dr. Francesca M. Rossi (CRO), for her valuable support for cytofluorimetric analyses.

Funding: This work was supported by a CRO Intramural grant (code J32F16001310007), by a grant received from the association "Finchè ci siete voi ci sono anch'io" (code J31I17000440007), by the organization "Alleanza Contro il Cancro (ACC)" (code J34I20000600001) and by "Associazione Italiana contro le Leucemie-linfomi e mieloma ONLUS (AIL)".

Footnote

Conflicts of Interest: All authors have completed the ICMJE uniform disclosure form (available at http://dx.doi.org/10.21037/atm.2020.04.25). The authors have no conflicts of interest to declare.

Ethical Statement: The authors are accountable for all aspects of the work in ensuring that questions related to the accuracy or integrity of any part of the work are appropriately investigated and resolved. Patients signed informed consent before enrolment. The study (protocol number: CRO-2016-30) was approved by the Ethics Committee of the Centro di Riferimento Oncologico di Aviano and it was compliant with the Helsinki Declaration.

References

1. Zuk PA, Zhu M, Ashjian P, et al. Human adipose tissue is a source of multipotent stem cells. Mol Biol Cell 2002;13:4279-95.
2. Agostini F, Rossi FM, Aldinucci D, et al. Improved GMP compliant approach to manipulate lipoaspirates, to cryopreserve stromal vascular fraction, and to expand adipose stem cells in xeno-free media. Stem Cell Res Ther 2018;9:130.

3. Samsonraj RM, Raghunath M, Nurcombe V, et al. Concise Review: Multifaceted Characterization of Human Mesenchymal Stem Cells for Use in Regenerative Medicine. Stem Cells Transl Med 2017;6:2173-85.
4. Dotoli GM, De Santis GC, Orellana MD, et al. Mesenchymal stromal cell infusion to treat steroid-refractory acute GvHD III/IV after hematopoietic stem cell transplantation. Bone Marrow Transplant 2017;52:859-62.
5. Introna M, Rambaldi A. Mesenchymal stromal cells for prevention and treatment of graft-versus-host disease: successes and hurdles. Curr Opin Organ Transplant 2015;20:72-8.
6. Markovic BS, Kanjevac T, Harrell CR, et al. Molecular and Cellular Mechanisms Involved in Mesenchymal Stem Cell-Based Therapy of Inflammatory Bowel Diseases. Stem Cell Rev Rep 2018;14:153-65.
7. Xie C, Yang Z, Suo Y, et al. Systemically Infused Mesenchymal Stem Cells Show Different Homing Profiles in Healthy and Tumor Mouse Models. Stem Cells Transl Med 2017;6:1120-31.
8. Dwyer RM, Khan S, Barry FP, et al. Advances in mesenchymal stem cell-mediated gene therapy for cancer. Stem Cell Res Ther 2010;1:25.
9. Uchibori R, Tsukahara T, Ohmine K, et al. Cancer gene therapy using mesenchymal stem cells. Int J Hematol 2014;99:377-82.
10. Krueger TEG, Thorek DLJ, Denmeade SR, et al. Concise Review: Mesenchymal Stem Cell-Based Drug Delivery: The Good, the Bad, the Ugly, and the Promise. Stem Cells Transl Med 2018;7:651-63.
11. Nitzsche F, Müller C, Lukomska B, et al. Concise Review: MSC Adhesion Cascade-Insights into Homing and Transendothelial Migration. Stem Cells 2017;35:1446-60.
12. Rüster B, Göttig S, Ludwig RJ, et al. Mesenchymal stem cells display coordinated rolling and adhesion behavior on endothelial cells. Blood 2006;108:3938-44.
13. Thankamony SP, Sackstein R. Enforced hematopoietic cell E- and L-selectin ligand (HCELL) expression primes transendothelial migration of human mesenchymal stem cells. Proc Natl Acad Sci USA 2011;108:2258-63.
14. Bailey AM, Lawrence MB, Shang H, et al. Agent-based model of therapeutic adipose-derived stromal cell trafficking during ischemia predicts ability to roll on P-selectin. PLoS Comput Biol 2009;5:e1000294.
15. Wynn RF, Hart CA, Corradi-Perini C, O'Neill L, et al. A small proportion of mesenchymal stem cells strongly expresses functionally active CXCR4 receptor capable of promoting migration to bone marrow. Blood 2004;104:2643-5.
16. Sackstein R, Merzaban JS, Cain DW, et al. Ex vivo glycan engineering of CD44 programs human multipotent mesenchymal stromal cell trafficking to bone. Nat Med 2008;14:181-7.
17. Ko KS, Arora PD, Bhide V, et al. Cell-cell adhesion in human fibroblasts requires calcium signaling. J Cell Sci 2001;114 Pt 6:1155-67.
18. Mazzucato M, Pradella P, Cozzi MR, et al. Sequential cytoplasmic calcium signals in a 2-stage platelet activation process induced by the glycoprotein Ibalpha mechanoreceptor. Blood 2002;100:2793-800.
19. Pfau S, Leitenberg D, Rinder H, et al. Lymphocyte adhesion-dependent calcium signaling in human endothelial cells. J Cell Biol 1995;128:969-78.
20. Agostini F, Polesel J, Battiston M, et al. Standardization of platelet releasate products for clinical applications in cell therapy: a mathematical approach. J Transl Med 2017;15:107.
21. Durante C, Agostini F, Abbruzzese L, et al. Growth factor release from platelet concentrates: analytic quantification and characterization for clinical applications. Vox Sang 2013;105:129-36.
22. Folie BJ, McIntire LV, Lasslo A. Effects of a novel antiplatelet agent in mural thrombogenesis on collagen-coated glass. Blood 1988;72:1393-400.
23. Schindelin J, Arganda-Carreras I, Frise E, et al. Fiji: an open-source platform for biological-image analysis. Nat Methods 2012;9:676-82.
24. Amos PJ, Bailey AM, Shang H, et al. Functional binding of human adipose-derived stromal cells: effects of extraction method and hypoxia pretreatment. Ann Plast Surg 2008;60:437-44.
25. D'souza N, Burns JS, Grisendi G, et al. MSC and Tumors: Homing, Differentiation, and Secretion Influence Therapeutic Potential. Adv Biochem Eng Biotechnol 2013;130:209-66.
26. Zhao Y, Zhang H. Update on the mechanisms of homing of adipose tissue-derived stem cells. Cytotherapy 2016;18:816-27.
27. Sensebé L, Gadelorge M, Fleury-Cappellesso S. Production of mesenchymal stromal/stem cells according to good manufacturing practices: a review. Stem Cell Res Ther 2013;4:66.
28. Parsons AM, Ciombor DM, Liu PY, et al. Regenerative Potential and Inflammation-Induced Secretion Profile of Human Adipose-Derived Stromal Vascular Cells Are

Influenced by Donor Variability and Prior Breast Cancer Diagnosis. Stem Cell Rev Rep 2018;14:546-57.
29. Kølle SF, Fischer-Nielsen A, Mathiasen AB, et al. Enrichment of autologous fat grafts with ex-vivo expanded adipose tissue-derived stem cells for graft survival: a randomised placebo-controlled trial. Lancet 2013;382:1113-20.
30. Chang YS, di Tomaso E, McDonald DM, et al. Mosaic blood vessels in tumors: Frequency of cancer cells in contact with flowing blood. Proc Natl Acad Sci U S A 2000;97:14608-13.
31. Huang Q, Hu X, He W, et al. Fluid shear stress and tumor metastasis. Am J Cancer Res 2018;8:763-77.
32. Semon JA, Nagy LH, Llamas CB, et al. Integrin expression and integrin-mediated adhesion in vitro of human multipotent stromal cells (MSCs) to endothelial cells from various blood vessels. Cell Tissue Res 2010;341:147-58.
33. Bonnans C, Chou J, Werb Z. Remodelling the extracellular matrix in development and disease. Nat Rev Mol Cell Biol 2014;15:786-801.
34. Dreher L, Elvers-Hornung S, Brinkmann I, et al. Cultivation in human serum reduces adipose tissue-derived mesenchymal stromal cell adhesion to laminin and endothelium and reduces capillary entrapment. Stem Cells Dev 2013;22:791-803.
35. Granger DN, Kubes P. The microcirculation and inflammation: modulation of leukocyte-endothelial cell adhesion. J Leukoc Biol 1994;55:662-75.
36. Ley K, Laudanna C, Cybulsky MI, et al. Getting to the site of inflammation: the leukocyte adhesion cascade updated. Nat Rev Immunol 2007;7:678-89.
37. Shamri R, Grabovsky V, Gauguet JM, et al. Lymphocyte arrest requires instantaneous induction of an extended LFA-1 conformation mediated by endothelium-bound chemokines. Nat Immunol 2005;6:497-506.
38. Wang JG, Geng JG. Affinity and kinetics of P-selectin binding to heparin. Thromb Haemost 2003;90:309-16.
39. Zarbock A, Ley K, McEver RP, et al. Leukocyte ligands for endothelial selectins: specialized glycoconjugates that mediate rolling and signaling under flow. Blood 2011;118:6743-51.
40. Ali AJ, Abuelela AF, Merzaban JS. An Analysis of Trafficking Receptors Shows that CD44 and P-Selectin Glycoprotein Ligand-1 Collectively Control the Migration of Activated Human T-Cells. Front Immunol 2017. doi:10.3389/fimmu.2017.00492.
41. Zhang K, Chen J. The regulation of integrin function by divalent cations. Cell Adh Migr 2012;6:20-9.
42. Jo CH, Ahn HJ, Kim HJ, et al. Surface characterization and chondrogenic differentiation of mesenchymal stromal cells derived from synovium. Cytotherapy 2007;9:316-27.
43. Roberts AI, Brolin RE, Ebert EC. Integrin alpha1beta1 (VLA-1) mediates adhesion of activated intraepithelial lymphocytes to collagen. Immunology 1999;97:679-85.
44. Shenkman B, Brill G, Solpov A, et al. CD4+ lymphocytes require platelets for adhesion to immobilized fibronectin in flow: role of beta(1) (CD29)-, beta(2) (CD18)-related integrins and non-integrin receptors. Cell Immunol 2006;242:52-9.
45. Phinney DG, Prockop DJ. Concise review: mesenchymal stem/multipotent stromal cells: the state of transdifferentiation and modes of tissue repair--current views. Stem Cells 2007;25:2896-902.
46. Yang J, Ren Z, Du X, et al. The role of mesenchymal stem/progenitor cells in sarcoma: update and dispute. Stem Cell Investig 2014. doi:10.3978/j.issn.2306-9759.2014.10.01.
47. Behnan J, Finocchiaro G, Hanna G. The landscape of the mesenchymal signature in brain tumours. Brain 2019;142:847-66.
48. Forner A, Reig M, Bruix J. Hepatocellular carcinoma. Lancet 2018;391:1301-14.
49. Jurisic G, Iolyeva M, Proulx ST, et al. Thymus cell antigen 1 (Thy1, CD90) is expressed by lymphatic vessels and mediates cell adhesion to lymphatic endothelium. Exp Cell Res 2010;316:2982-92.
50. Ponta H, Sherman L, Herrlich PA. CD44: from adhesion molecules to signalling regulators. Nat Rev Mol Cell Biol 2003;4:33-45.
51. van Kempen LC, Nelissen JM, Degen WG, et al. Molecular basis for the homophilic activated leukocyte cell adhesion molecule (ALCAM)-ALCAM interaction. J Biol Chem 2001;276:25783-90.
52. Sitrin RG, Todd RF, Albrecht E, et al. The urokinase receptor (CD87) facilitates CD11b/CD18-mediated adhesion of human monocytes. J Clin Invest 1996;97:1942-51.
53. Sándor N, Lukácsi S, Ungai-Salánki R, et al. CD11c/CD18 Dominates Adhesion of Human Monocytes, Macrophages and Dendritic Cells over CD11b/CD18. PLoS One 2016;11:e0163120.
54. Bourin P, Bunnell BA, Casteilla L, et al. Stromal cells from the adipose tissue-derived stromal vascular fraction and culture expanded adipose tissue-derived stromal/stem cells: a joint statement of the International Federation for Adipose Therapeutics and Science (IFATS) and the International Society for Cellular Therapy (ISCT).

Cytotherapy 2013;15:641-8.
55. Lee TC, Lee TH, Huang YH, et al. Comparison of surface markers between human and rabbit mesenchymal stem cells. PLoS One 2014;9:e111390.
56. Gronthos S, Franklin DM, Leddy HA, et al. Surface protein characterization of human adipose tissue-derived stromal cells. J Cell Physiol 2001;189:54-63.
57. Serejo TRT, Silva-Carvalho AÉ, Braga LD de CF, et al. Assessment of the Immunosuppressive Potential of INF-γ Licensed Adipose Mesenchymal Stem Cells, Their Secretome and Extracellular Vesicles. Cells 2019. doi:10.3390/cells8010022.
58. Ren G, Zhao X, Zhang L, et al. Inflammatory cytokine-induced intercellular adhesion molecule-1 and vascular cell adhesion molecule-1 in mesenchymal stem cells are critical for immunosuppression. J Immunol 2010;184:2321-8.
59. Resende RR, Adhikari A, da Costa JL, et al. Influence of spontaneous calcium events on cell-cycle progression in embryonal carcinoma and adult stem cells. Biochim Biophys Acta 2010;1803:246-60.
60. Pinto MCX, Kihara AH, Goulart VAM, et al. Calcium signaling and cell proliferation. Cell Signal 2015;27:2139-49.
61. Gaudenzio N, Sibilano R, Marichal T, et al. Different activation signals induce distinct mast cell degranulation strategies. J Clin Invest 2016;126:3981-98.
62. Savina A, Furlán M, Vidal M, et al. Exosome release is regulated by a calcium-dependent mechanism in K562 cells. J Biol Chem 2003;278:20083-90.
63. Smedler E, Uhlén P. Frequency decoding of calcium oscillations. Biochim Biophys Acta 2014;1840:964-9.
64. Bang OY, Kim EH. Mesenchymal Stem Cell-Derived Extracellular Vesicle Therapy for Stroke: Challenges and Progress. Front Neurol 2019. doi:10.3389/fneur.2019.00211.
65. Varkouhi AK, Jerkic M, Ormesher L, et al. Extracellular Vesicles from Interferon-γ-primed Human Umbilical Cord Mesenchymal Stromal Cells Reduce Escherichia coli-induced Acute Lung Injury in Rats. Anesthesiology 2019;130:778-90.
66. Kumar JD, Holmberg C, Balabanova S, et al. Mesenchymal Stem Cells Exhibit Regulated Exocytosis in Response to Chemerin and IGF. PLoS One 2015. doi:10.1371/journal.pone.0141331.

Cite this article as: Agostini F, Vicinanza C, Di Cintio F, Battiston M, Lombardi E, Golinelli G, Durante C, Toffoli G, Dominici M, Mazzucato M. Adipose mesenchymal stromal/stem cells expanded by a GMP compatible protocol displayed improved adhesion on cancer cells in flow conditions. Ann Transl Med 2020;8(8):533. doi: 10.21037/atm.2020.04.25

Supplementary

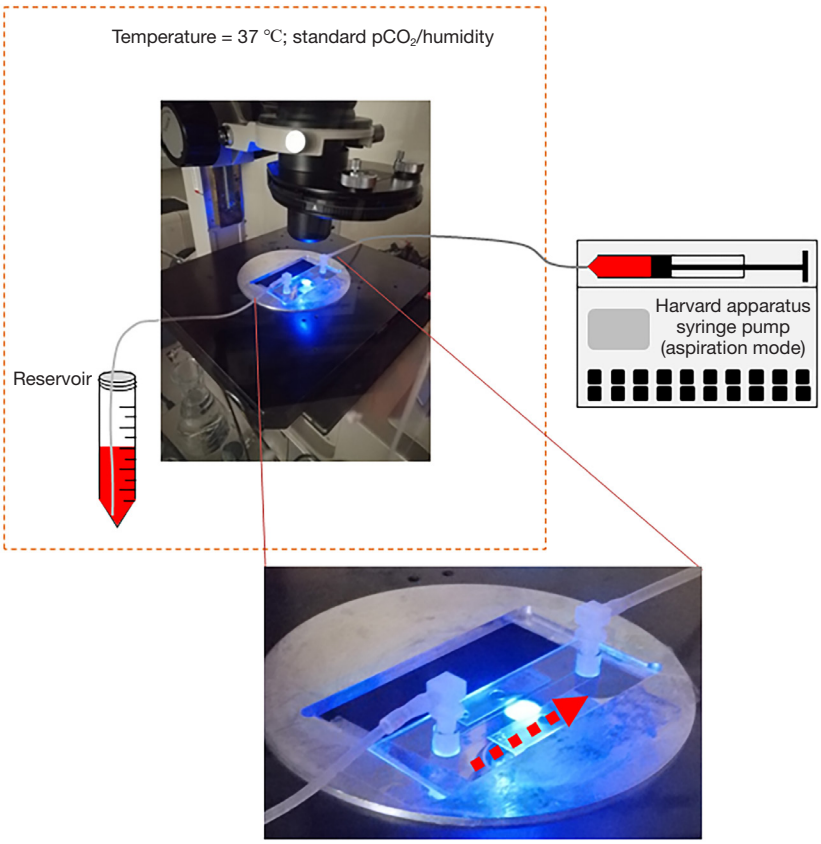

Figure S1 Schematic representation of devices used to perform ASC adhesion and detachment assays. The parallel flow chamber slide (see photographic enlargement), was placed on an inverted epifluorescence microscope. Washed ASC after fluorescent labeling were resuspended with perfusion medium in a conical tube (Reservoir). In controlled environment (37 °C; standard atmospheric pCO_2 and humidity) ASC were perfused in the parallel flow chamber through a small bore catheter. Flow was imposed by a syringe pump (Harvard apparatus). Adherent and detaching ASC were visualized by a digital camera and the number of adherent cells was estimated by image analysis approach. Timing of flow rate regulation and of digital image capture was reported in methods section and in *Figure 1A*. Dashed arrows represent the direction of flowing medium containing labeled ASC. Dashed orange box encloses devices placed under controlled environmental conditions.